

September 27, 1964

north of the array. The relative velocity of the main currents and the low frequency wave motions do not account for the observed shift of the near-intrinsic frequencies ~75 above it. An advent of turbulence near-bottom may explain the shift. The passage of Balla appears to be attributable to currents (amplitude ~ 10 cm at Balla) (August 5-10, 1976) 24 days after the passage of Hurricane Berta. The vertical travel time are also fairly primarily the estimates of vertical group velocity. Strongly (~40 cm/sec), deep currents north of the array (amplitude ~ 10 cm/sec) during hurricane Balla were observed at the shear edge (August 18-19, 1976) with peak frequencies comparable to the near-intrinsic frequencies observed at the array on the rise. Boundary layer and exchange processes, internal waves.

J. Gougho, Soc., Ocean, Paper C1472

4799 Inouae (Polypnea)
NATURALIST OBSERVED BEHAVIOR OF THE TINKLEWILL
Dennis B. Ruten and David W. Bromell (Editor of
Polar Studies, Ohio State University, Columbus, Ohio)

Infrared satellite images indicate that the glacier
surrounded by a zone of warm water, ice, permafrost
and icebergs. The glacier, through the water, is affected
by the fracture may occur during, roughly 1980 to 1985
(Polypnea and Bromell). The glacier is roughly 1980 to 1985
and 1985 to 1985. The glacier is roughly 1980 to 1985
open water (flooded) (ice-bergs) (ice-bergs) (ice-bergs)
of 400 days (ice-bergs) (ice-bergs) (ice-bergs) (ice-bergs)
are approximately 1980 to 1985. The glacier is roughly
associated with the magnitude of the glacier is roughly
of 400 days (ice-bergs) (ice-bergs) (ice-bergs) (ice-bergs)
invariant condition. An open, or open, or open, or open,
invariant condition. An open, or open, or open, or open,
linked with persistent water. The glacier is roughly
of 400 days (ice-bergs) (ice-bergs) (ice-bergs) (ice-bergs)
drift-bearing air from the glacier. The glacier is roughly
of 400 days (ice-bergs) (ice-bergs) (ice-bergs) (ice-bergs)
Peters have Bay through the glacier. The glacier is roughly
of 400 days (ice-bergs) (ice-bergs) (ice-bergs) (ice-bergs)
probably due to the action of the glacier. The glacier is roughly
wind, white air from the glacier. The glacier is roughly
and back to the glacier. The glacier is roughly
animals advancing far toward and away from the glacier.
(See also, Polypnea, Infrared satellite images, Polypnea)

3280 Soter wind plasma
SHORT-WAVELENGTH LOW WAVES UPSTREAM OF THE KATY
SHOCK
S. A. Fuselier (Dept. of Physics and Astronomy, The
University of Iowa, Iowa City, IA 52242) and J. E.
Gurnett
The identification and explanation of short w-

[illegible]

budget of \$6.8 billion. President Ronald Reagan signed the budget into law (P.L. 96-32) on July 15. The lion's share—\$5.9 billion—of the NASA budget goes to research and development (see Table 1). NASA officials, using the authorizing levels as a strict guide, distributed the funds to the various programs (see Table 2). NASA must ask congressional appropriations committees to approve the minor discrepancies between this distribution and the authorizing legislation. Among such discrepancies: The physics and astronomy subactivity was authorized for \$562.1 million, but NASA officials set a program level of \$567.6 million. NASA set the program level for planetary exploration, authorized for \$220.4 million, at \$217.4 million.

Eos will review the National Science Foundation budget in a coming issue.—BTR

Activity	Reagan Proposal ¹	House Version ²	Senate Version ³	Authorization
Space Transportation Systems				
Capability development	1927.4	2001.2	2009.4	2009.4
Operations	1570.6	1570.6	1545.6	1545.6
Subtotal	3498.0	3571.8	3555.0	3555.0
Space Science & Applications				
Physics & astronomy	514.6	566.6	562.1	562.1
Planetary exploration	205.4	220.4	220.4	220.4
Life sciences	59.0	59.0	59.0	59.0
Space applications ⁴	396.14	396.0	313.0	313.0
Subtotal	1098.0	1162.0	1154.5	1154.5
Technology Utilization	4.0	10.0	10.0	10.0
Aeronautics & Space Technology⁵				
Aeronautics	310.3	311.5	320.3	320.3
Space Technology	138.0	143.0	143.0	143.0
Subtotal	438.3	454.6	433.3	433.3
Tracking & Data Acquisition	700.2	700.2	700.2	700.2
Total Research & Development	5708.5	5888.3	5883.0	5883.0

¹Source: NASA. Numbers may not total because of rounding.
²See *Eow*, February 13, 1983, p. 65.
³Trans H.R. 2005, which passed the House of Representatives on April 26. See also *Eow*, May 17, 1983, p. 378.
⁴Passed by the Senate on June 28.
⁵Signed into public law (PL) 100-52 on July 13.
⁶Includes solid earth observations, environmental observations, materials processing in space communications, and information systems.

phenomena are currently one of the main areas of superfluid research in the laboratory.

At one atmosphere, liquid helium becomes a superfluid at 2.17 K. At the other extreme, in the interiors of pulsar stars, for example, helium becomes superfluid at incredibly high densities even though the temperature is extremely high—more than one million degrees. It could be that this superfluid behaviour affects the timing of radiation emission of pulsars. Baird et al. showed in laboratory experiments that the interaction between phonons and surface atoms in liquid helium is a "one-to-one" quantum process. These results and other work on superfluids could form a basis for understanding the evaporation and melting processes of condensed matter on the microscopic scale.—*PMB*

The federal government distinguishes three types of activity under the title Research and Development (R&D), which was budgeted at \$45.8 billion for 1984: basic research, applied research, and development. According to the National Science Foundation, the 1984 federal R&D obligation is 5 times the 1974 level. While the apparent 10-year growth of the R&D budget was about 10.2% per year in current dollars, real annual growth averaged only 2.5%. Moreover, averages themselves are misleading because most of the growth has taken place since 1981, mostly in defense programs.

The basic research portion of the R&D budget is \$6.8 billion, one-third of which is allocated to biomedical research areas administered through the National Institutes of Health. However, the Department of Health and Human Services budget showed a real-dollar decline in 1984 of 3%. By contrast, the National Science Foundation budget, a portion of which also is granted for biological research, showed a less rapid rate of growth between 1974 and 1983, but had

Activity	Fiscal 1983	Reagan Proposal ¹	NASA FY 1984 Program Level
Physics & Astronomy			
Space telescope development	187.5	120.0	195.6
Gamma Ray Observatory (GR1)	34.5	89.8	86.2
Shuttle/spacecraft payload development & mission management	88.0	102.9	80.0
Explorer development	34.3	48.7	48.7
Mission operations & data analysis	74.8	79.5	68.1
Research & analysis	28.8	29.8	33.8
Suborbital program	48.1	53.3	52.3
Subtotal	441.0	514.6	967.8
Planetary Exploration			
Galileo development	91.6	79.5	70.5
Venus Radar Mapper (VRM)	0	29.0	29.0
International Solar Polar Mission	6.0	8.0	6.0
Mission operations & data analysis	38.5	43.1	43.4
Research & Analysis	50.3	45.5	50.5
Subtotal	186.4	205.4	217.4
Life Sciences	35.7	59.0	58.0
Solid Earth Observations			
Landsat 4	61.7	15.8	16.8
Shuttle/spacecraft payloads	13.8	15.0	16.0
Geodynamics	26.2	28.0	21.5
AgRISTARS ²	15.0	0	0
Research & analysis	13.7	14.6	14.6
Other ³	1.8	1.0	7.5
Subtotal	132.2	74.4	73.4
Environmental Observations			
Shuttle/spacecraft payload development	3.7	7.6	7.6
Operational satellite improvement program	6.0	0.0	0.0
Earth radiation budget experiment	24.0	13.5	15.5
Extended mission operations	22.8	27.4	27.4
Upper atmosphere research satellite experiments & mission definition	14.0	20.0	20.0
Research & analysis ⁴	86.4	91.0	100.0
Subtotal	159.9	163.0	192.0
Materials Processing in Space	22.0	21.6	23.6
Communications	32.4	21.1	21.1
Information Systems	7.5	8.9	8.9
Total, Space Science & Applications	1034.1	1068.0	1154.0

Source: NASA. Numbers may not total because of rounding.
See Eos, February 15, 1983, p. G5.
 *These figures are program levels as distributed by NASA using the authorization levels (Table 1) as a guideline. NASA must seek approval from congressional appropriations committees for those program distributions that differ from the authorization levels.
 *AgRISARS continued in fiscal 1983.
 †Includes extended mission operations and laser network operations.
 ‡Includes research and analysis for upper atmosphere, atmospheric dynamics and radiation-ocean processes, and space physics programs.

Streamflow conditions in the far west remained in the above-normal range during August, with well above average flows reported from southern Washington south through California and as far east as central Colorado.

In sharp contrast to the far west, extreme low-flow conditions persisted in parts of the Great Plains states, and the below-average flows that were reported only in scattered areas of the Southeast in July extended throughout the mid-Atlantic and southeast during August, according to the U.S. Geological Survey (USGS) (see map, courtesy of USGS).

USGS hydrologists said that the combined flow of the nation's three largest rivers—the Mississippi, St. Lawrence, and Columbia—reflected the contrast in the water picture, with the unusually high flows of the west, balanced by the many low flows in the east. During August, the combined flow was 223.7 billion liters per day (60 billion gallons a day), only 5 percent above the average and down 33 percent from July's combined flow. These three major rivers drain more than half of the conterminous United States and serve as a useful guide to the status of the nation's water resources.

Flows at the 172 key index gaging stations recorded by the USGS during August showed that 69 stations (37%) recorded streamflows

Atmospheric Sciences

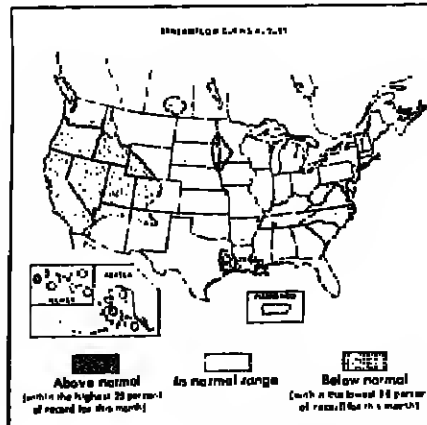
Doron in the Marine Atmosphere, Thomas R. Fogg, Center for Atmospheric Chemistry Studies, Graduate School of Oceanography, Univ. of Rhode Island, May 1983.

The Effects of Long-Range Transport of Air Pollutants on Arctic Cloud-Acid Aerosol, Randolph D. Borys, Dept. of Atmospheric Science, Colorado State Univ., May 1983.

Hydrology

River Basin Water Quality Monitoring Network Design, Franklin S. Tiruch, Dept. of Civil Engineering, Univ. of Massachusetts-Amherst, May 1983.

A Mirman-Weibull Model of Hydrologic Drought in the Farmington River Basin of Connecticut and Massachusetts, Richard James Dalphin, Environmental Engineering, Univ. of Connecticut, June 1983.



The Oceanography Report



The Oceanography Report
The focal point for physical, chemical, geological, and biological oceanography.

Editor: Arnold L. Gordon, Lamont-Doherty Geological Observatory, Palisades, NY 10964 (telephone 914-359-2900, ext. 325).

MIZEX West: Bering Sea Marginal Ice Zone Experiment

MIZEX West Study Group¹

Introduction

The most thorough field study of the Bering Sea Marginal Ice Zone (MIZ) attempted to date was conducted February 5-27, 1983. This study, MIZEX West, was part of a larger program addressing processes which control interactions among the atmosphere, ice, and ocean in the northern hemisphere MIZs (Muench, 1983a). The other part of this overall program, MIZEX East, addresses processes in the Greenland Sea MIZ (Muench, 1983b).

MIZEX West is an interdisciplinary, multi-institutional program that addresses a broad spectrum of physical problems related to the Bering Sea MIZ. Oceanographic studies attempt to measure and explain dynamically the frontal structure associated with the ice edge. Sea ice studies address the dynamic processes which control ice movement, ice interactions, and melting. Meteorological data contribute to knowledge of wind stress transfer through an ice cover and development of atmospheric boundary layers. Remote sensing information contributes to knowledge of the ice cover and enhances our ability to apply aircraft- or satellite-acquired data to the study of Arctic regions. This article summarizes the goals, methods, and some preliminary results from MIZEX West.

The MIZEX West program took place along the central Bering Sea MIZ (Figure 1). This program consisted of an intensive field experiment in the vicinity of and north of the ice edge February 5-27, 1983, during the time of maximum ice extent and most rapid growth. The winter experiment employed the following research platforms:

(1) The NOAA Ship *Discoverer*. This vessel was equipped with a conductivity/temperature/depth (CTD) sensing system and with instrumentation for both surface meteorological and upper air observations. It was used as a base for deployment of personnel and remote instrumentation onto the ice, and housed equipment for recording data from these instruments and tracking them. With an ice-strengthened hull, the *Discoverer* was able to work in the relatively loose, broken ice in and near the ice edge.

(2) The U.S. Coast Guard icebreaker *Westwind*. This ship was equipped with oceanographic and meteorological instrumentation similar to that on the *Discoverer* and was likewise used to deploy personnel and instrumentation onto the ice. In addition, *Westwind* had two helicopters which were used for gear and personnel deployment and recovery at locations near the ship. These helicopters

were essential for such experiments as the wave attenuation experiment summarized below. The icebreaking capability of *Westwind* allowed it to operate in the relatively solid ice well north of the edge, where *Discoverer* could not penetrate.

(3) The NOAA WP-3D Research Aircraft. This aircraft was based in Anchorage, Alaska, and overflew the experiment five times. The aircraft was equipped with gust probes to measure atmospheric turbulence and a SLAR (side-looking air radar), laser altimeter, and cameras to observe ice properties. The WP-3D flew over the study region at altitudes between 50 and 1500 m.

(4) The NASA CV-990 Airborne Laboratory. The NASA aircraft, which was also based in Anchorage, was equipped with several passive microwave radiometers, an infrared radiometer, two photographic cameras, and a version of the radar altimeter planned for the European Space Agency satellite ERS. The aircraft made five mosaic flights over the research area at an altitude of 10,000 m. Visual and photographic records of the general ice characteristics also made during the flights provided supporting data for interpreting the microwave measurements.

Information obtained from these four platforms was supplemented with current and other data from four moorings (Figure 1) which were deployed in October 1982 and recovered in May 1983 using the University of Alaska research vessel *Alpha Helix*.

The above research platforms and instrumentation constituted the MIZEX West core field program. Additional CTD data were obtained from the study area during the period from February 20 to March 18 using the U.S. Coast Guard icebreaker *Polar Sea*. Imagery was also obtained routinely from both the Nimbus and NOAA satellites. Finally, the National Weather Service office in Anchorage, Alaska provided real-time surface weather maps and ice distribution charts.

The Scientific Program Oceanographic Studies

The oceanography portion of the program focused upon improving understanding of the oceanic frontal structure associated with the Bering Sea ice edge (Muench, 1983b). To this end, four moored current moorings were deployed at locations (Figure 1) which bracketed the winter ice edge. Depths of current observation (Figure 2) were selected so as to measure currents in the upper and lower layers and near the frontal transition, as illustrated in Figure 6. In addition to the current

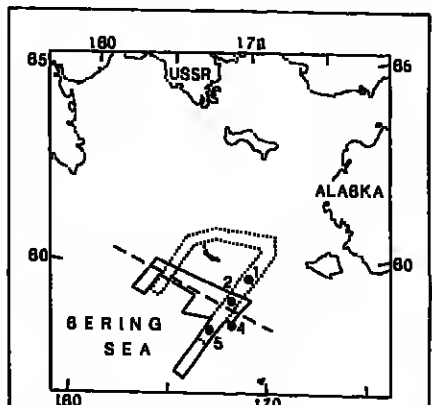


Fig. 1. Geographical location of the MIZEX West operations area. Solid line encompasses the area covered by the NOAA Ship *Discoverer*. Dotted line encloses the area covered by the Coast Guard icebreaker *Westwind*. Numbered dots show locations of current moorings. Dashed line indicates approximate ice edge location during the experiment.

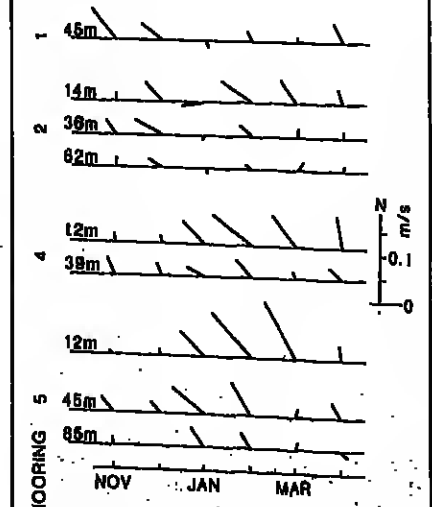


Fig. 2. Monthly vector-averaged currents obtained from the MIZEX West moorings. Mooring locations are shown in Figure 1 and depths of observations are given in meters at the left end of each time-axis.

rent meters, bottom-mounted pressure gauges were deployed at moorings 1, 2, and 3 to measure fluctuations in the cross-shelf pressure field. The near-surface meters at moorings 2, 4, and 5 were vector-averaging acoustic current meters; the remaining current meters were Savonius rotor units.

To augment the current data, temperature (T) and salinity (S) transects were made across the ice edge from three different vessels from February 5 through March 18. These T and S data were sufficient to estimate mesoscale temperature and salinity features associated with the midwinter ice edge. The CTD data were supplemented with time-series of temperature obtained from each of the current meters and pressure gauges and with salinity data from the middepth current meters at moorings 2, 4, and 5. In addition to the winter data, CTD data were obtained from the study region in October 1982 and May 1983 during the deployment and recovery of the current moorings.

The current and CTD data obtained during MIZEX West provided excellent definition of the ice-edge-associated oceanic frontal structure. Figure 3 shows preliminary results from the current meters. The high, north-northwestward, near-surface current speeds associated with the ice edge front in February and March are apparent. These speeds were highest (nearly 0.15 m s⁻¹) in March at mooring 5, at a time and location where ice melting would be expected to contribute maximum freshwater input (hence baroclinic driving for the ice edge current) to the water column. Also apparent is the regional mean northwesterly flow which persisted throughout the mooring period.

The CTD data substantiated the frontal structure described for the Bering Sea ice edge region by Muench (1983a) and shown schematically in Figure 6. These data were adequate, moreover, to define temporal fluctuations in the T and S fields and to greatly improve existing documentation of regional winter T and S distributions.

Wave-Ice Interaction Studies

The energy loss suffered by ocean waves traveling through Bering Sea pack ice was studied during three experiments that took place from *Westwind*. The importance of these waves lies in their ability to form the large internal flows into smaller flows which are typical of the MIZ. In each experiment the wave-induced vertical acceleration (heave) of ice floes was measured along a line in the direction of the principal swell as observed from *Discoverer*. Whenever possible, the station separation was chosen to be the maximum possible within the constraints of helicopter range. The data were collected by vertical accelerometers allowed to record for 20 minutes at each successive location.

Preliminary power spectral analyses of the vertical acceleration data have revealed that ocean waves present during each experiment were at unusually low periods (Figure 3). The lowpass filtering effect of the ice cover could be clearly seen in the data, as spectral peaks became narrower with increasing distance from the ice edge. The decay of significant wave height with distance from the ice edge (Figure 4) was measured along the most southerly station in a given transect as shown in Figure 4. There is excellent agreement between the observed wave attenuation and a simple exponential decay law.

Ice Dynamics Studies

Sea ice motion in the MIZ was measured with three different sets of buoys deployed from both *Westwind* and *Discoverer*. A set of four radar-tracked buoys deployed on the ice from *Westwind* had horizontal separations ranging from 0.5 to 5 km and was tracked at 0.5-hr intervals over an 11-day period using the LORAN-C and the radar range and bearing of each buoy. This radar-tracked array was nested inside a second triangular array of eight satellite-tracked ARGOS buoys with separations of 10 to 40 km (Figure 5). These buoys drifted westward approximately 350 km in 14 days, while the ice edge advanced 90 km. Two of the array sites were equipped with an accelerometer, current meter, and air and water thermistors; these data were recovered from the drift data with 10-m winds shows that the ice floes initially drifted at 4% of the wind speed within 30 km of the ice edge.

A similar series of ice drift and deformation experiments was done in the ice edge region from *Discoverer*. These experiments documented further the rapid drift and divergent ice field near the ice edge.

The radar transponder drift buoys each contained tri-axial accelerometers which measured vertical and horizontal accelerations of the ice floes in the 0.5 to 20 s range. These accelerations were transmitted for 20 minutes out of each hour to the ships for recording. The acceleration data show both propagation of ocean swell into the pack and high-frequency ice collisions.

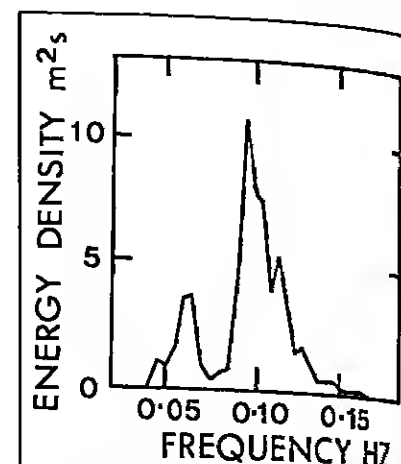


Fig. 3. Energy spectrum from a buoy deployed on an ice floe 15 km from the ice edge. The primary energy peak at 0.10 Hz is due to a locally wind-generated sea. The secondary, 0.08-second (12.5 Hz) peak reflects swell propagating into the region from the North Pacific.

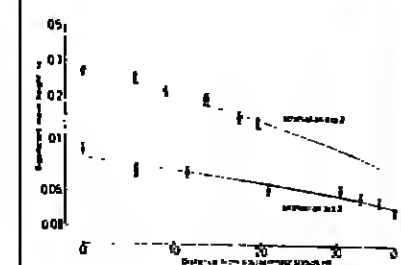


Fig. 4. Decay of significant wave height with increasing distance into the ice for two separate experiments.

buoys were instrumented along the edge to test the hypotheses of Muench (1983) and Martin et al. (1983) that locally wind-generated waves heave the ice edge along the edge into basins, then drive these basins in a downwind direction to effectively increase ice divergence at the edge. The results confirmed the effectiveness of this mechanism. Two other classes of ice edge bands were also observed. In at least one instance a band was parallel to, and apparently caused by, the wind field associated with an atmospheric vortex, as suggested by Muench and Chinn (1977). Additional bands were observed which had formed from a regular array of narrow leads which opened normal to the wind direction. A marked circulation of individual ice floes internal to each band was observed. This circulation was capable of incorporating floes (or small basins) along the leeward edge of the band rapidly into the band interior.

Ice Edge Ablation

One of the major contributors to the ice edge salt and heat balance is the melting of ice floes as the wind advects them south across the front into warmer water. To study this melting, an ice floe measuring about 20 m by 40 m was instrumented with melt gauges over a 1.2-m thick, smooth portion of the floe. The floe was also instrumented with a current meter, an unmoored meter, and a radar transponder. It was then tracked over a 24-hour period as northwest winds blew the floe into warmer water at speeds of up to 0.8 m s⁻¹.

The floe was initially in sea water at -1.5°C. Over the next 24 hours the water temperature increased from -1.5°C to 0°C and the observed bottom melt rate was 7 mm hr⁻¹. Over the next 20 hours the water temperature increased to +1.0°C, and the melt rate increased to 20 mm hr⁻¹. Over the entire 44-hour experiment, the ice thickness decreased by 0.6 m. At the same time, the floe was carried into near-open water and suffered severe erosion at the top and sides from waves washing over the top. This lateral erosion and the top erosion increased as the water temperature increased owing to floe advection and wave erosion at the sides and edges supports the idea derived from previous cruises (that the +1.0°C isotherm is the boundary between open water and ice. The data acquired will allow testing of theories by Josberger (1983) and Muench (1983b) concerning ice melting.

Meteorological Observations

The meteorological observation program focused on boundary layer processes associated with passage of air from the ice cover over open water and upon vertical fluxes of heat, moisture, and momentum. Surface observations obtained from both vessels and from aircraft were used to estimate the boundary layer fluxes of heat, moisture, and momentum. Upper-air observations taken from both vessels included temperature and humidity. Five flights of the WP-3D Research Aircraft allowed estimation of vertical fluxes of heat, moisture, and momentum. Upward- and downward-looking radiance measurement devices were used to estimate radiative fluxes.

The data obtained appear adequate to constrain an atmospheric heat budget for the MIZ region. The meteorological conditions which prevailed through the field program (northeast winds blowing off-ice) yielded strong boundary layer development along the ice edge. Hence the data are expected to be useful for testing a hypothesis proposed for MIZ boundary layer development by Overland et al. (1983). Combined wind, ice, and water motion observations should also be adequate to test previous drag coefficient values reported by Pease et al. (1983) and Macklin (1983).

Remote Sensing Studies

A major goal of the remote sensing program is to study microwave radiometric properties of the Bering MIZ for the purpose of further improving sea ice concentration retrievals from space observations. Although passive microwave techniques have a proven ability to provide useful sea ice observations under all conditions of weather and seasons, there are still unresolved problems which limit significantly the accuracy of calculated ice concentrations (Cavalieri et al., 1983). This is especially the case in the marginal ice zones, which are characterized by new ice production and growth and by rapid ice type changes. The problem is to resolve ambiguities that are associated with the presence, within the field-of-view of the instrument, of open water and of new, young, and thin first-year ice types. Variations in ice type coverage are suspected to result in false concentration gradients within both the ice-edge zone and interior pack.

One approach in resolving this problem will be to examine the polarization and spectral characteristics of the ice cover at wavelengths ranging from millimeter to centimeter in order to obtain distinctive microwave signatures for each of the various species of first-year sea ice. Data from both airborne and spacecraft sensors will be used for this purpose. The aircraft's 0.33-cm wavelength

imaging radiometer, for example, gives excellent definition of the ice edge, ice bands, and areas of open water within the pack. Variations of brightness temperature from consolidated pack ice presumably reflect variations of surface characteristics associated with different ice types. Other approaches to this problem will include combined active/passive studies employing selected passive microwave wavelengths and radar altimeter returns.

Preliminary results from a comparison of Nimbus II satellite microwave imagery with aircraft observations confirm that the satellite correctly locates the ice edge position and the regions of low ice concentration associated with ice shore polynyas (see cover figure). However, a significant fraction of the concentration gradients within the interior pack derived from satellite data results from spatial variations of ice type. In the cover figure, for instance, currently calculated ice concentrations of 85% or greater are associated with a first-year thin or medium ice cover; concentrations between 65% and 85% are associated with young ice; and concentrations below 55% are associated with new ice. Further analysis, however, has shown that the 0.81-cm polarization can distinguish among new, young, and first-year sea ice. This result holds promise for the discrimination of these first-year ice types. We hope that further analysis using other wavelengths will uncover distinctive spectral signatures needed to identify unambiguously each of the ice types. Analysis of surface radiometric measurements and ice core results, obtained from both ships, should help confirm these early observations.

Summary

Figure 6 summarizes the observations from MIZEX West. The buoy drift results suggest that the MIZ divides into two parts: region I, where ice motion at the 1-5 km scale is nearly solid body (i.e., is nearly that of a single mass) and where "leads" (irregular, ice-free areas) typically fill with ice; and region II, where the ice disperses in a near-random motion superimposed on the wind-driven displacement.

The region in which ice dispersion occurs is over the geographic current shear region associated with the ice edge front. Across this zone, the sea water temperature increases from the freezing point to approximately +1°C. The ice is broken up by ocean swell propagating into the pack and melts in the warmer water. At the same time, turbulent fluxes associated with winds and currents deform and stretch the masses of ice into filaments or bands. Wind waves generated on the open water accelerate these bands into the warmer water. There is a melting over this two-layered system contributes to upper layer stability and helps maintain the alongfront geostrophic flow.

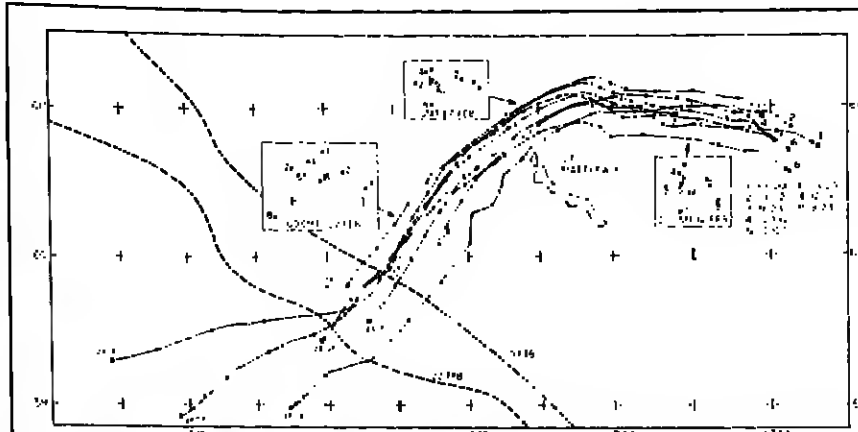


Fig. 5. Drift tracks for the eight ARGOS buoys deployed on the ice from *Westwind*. Dashed lines show approximate ice locations on February 10 and 22. Numbers at the beginning and end of track give the day counting from February 1 (UT). RCVD indicates recovery of the buoy.

As the wind blows over the open water of region II, the surface conditions change from cold ice to warm water. The corresponding flux of heat into the atmosphere creates a rapidly developing, unstable boundary layer which leads to the formation of roll vortices aligned approximately parallel to the wind and additional turbulence at the ocean surface.

Acknowledgments

Core support for the MIZEX West program has been provided by the Office of Arctic Programs, Office of Naval Research. Additional support has been provided by the National Oceanic and Atmospheric Administration, the National Aeronautics and Space Administration, The National Science Foundation, and the U.S. Geological Survey.

References

- Cavalieri, D. J., S. Martin, and P. Gloersen. Nimbus II SMMR observations of the Bering Sea ice cover during March 1979. *J. Geophys. Res.*, 88, 2713-2724, 1983.
- Josberger, E. G. Sea ice melting in the Marginal Ice Zone. *J. Geophys. Res.*, 88, 2841-2844, 1983.
- Macklin, S. A. Wind drag coefficient over first-year sea ice in the Bering Sea. *J. Geophys. Res.*, 88, 2845-2852, 1983.
- Martin, S. P., K. Lindstrom, and C. Parkinson. The movement and decay of ice edge bands in the winter Bering Sea. *J. Geophys. Res.*, 88, 2803-2812, 1983.
- McPhee, M. G. Greenland Sea ice/ocean margin. *Geophys. Res. Lett.*, 6, 82-83, 1983.
- McPherson, M. G. Turbulent heat and momentum transfer in the ocean boundary layer under melting pack ice. *J. Geophys. Res.*, 88, 2827-2835, 1983.
- Muench, R. D. MIZEX. The Marginal Ice Zone Experiment. *Oceanus*, 26, 55-60, 1983a.
- Muench, R. D. Mesoscale oceanographic features associated with the central Bering Sea ice edge: February-March 1981. *J. Geophys. Res.*, 88, 2715-2722, 1983b.
- Muench, R. D., and R. L. Chinnell. Observations of medium-scale features along the seasonal ice edge in the Bering Sea. *J. Phys. Oceanogr.*, 13, 602-606, 1977.
- Overland, J. E., R. M. Reynolds, and T. H. Persse. A model of the atmospheric boundary layer over the Marginal Ice Zone. *J. Geophys. Res.*, 88, 2836-2840, 1983.
- Pease, C. H., S. A. Salo, and J. E. Overland. Drag measurements for first-year sea ice over a shallow sea. *J. Geophys. Res.*, 88, 2853-2862, 1983.
- Wadhams, P. A mechanism for the formation of ice edge bands. *J. Geophys. Res.*, 88, 2813-2818, 1983.

Christmas Island Birds Returning

Six months after their mass exodus, birds are beginning to return to Christmas Island. Roughly 17 million birds, almost the entire adult bird population, either perished or fled their mid-Pacific atoll home last autumn, leaving behind thousands of nestlings to starve (EOS, April 5, 1983, p. 131). It is believed that the strong El Niño altered the ecology of the surrounding waters and forced the birds to flee. Christmas Island is the world's largest coral atoll.

Ocean and atmosphere scientists are unsure of future directions for the El Niño conditions and cannot now predict what will happen to the birds in the coming months," said Ralph W. Schreiber, curator of ornithology at the Natural History Museum of Los Angeles County in California. He is the ornithologist who discovered the disappearance. "The recovery of the bird populations depends on the food supply in the waters surrounding the island." The island's birds feed exclusively on small fish and squid.

As part of a survey on the biology of tropical seabirds as affected by the El Niño, Schreiber returned to the island for 10 days in June to survey the bird population. He reports that individuals representing most of the 18 species that fled have returned in small numbers. Three species are breeding at a rate approaching pre-exodus levels.

ATTENTION NON-U.S. MEMBERS

To speed your book or journal orders use AGU's

TWX number

TWX 710-822-9300

7 days a week

24 hours a day

EOS

